

How early is early dark energy?

Valeria Pettorino¹, Luca Amendola², Christof Wetterich²

¹ *Département de Physique Théorique and Center for Astroparticle Physics,
Université de Genève, 24 quai Ernest Ansermet, CH-1211 Genève 4, Switzerland.*

² *Institut für Theoretische Physik, Universität Heidelberg,
Philosophenweg 16, D-69120 Heidelberg, Germany.*

(Dated: September 12, 2018)

We investigate constraints on early dark energy (EDE) from the Cosmic Microwave Background (CMB) anisotropy, taking into account data from WMAP9 combined with latest small scale measurements from the South Pole Telescope (SPT). For a constant EDE fraction we propose a new parametrization with one less parameter but still enough to provide similar results to the ones previously studied in literature. The main emphasis of our analysis, however, compares a new set of different EDE parametrizations that reveal how CMB constraints depend on the redshift epoch at which Dark Energy was non negligible. We find that bounds on EDE get substantially weaker if dark energy starts to be non-negligible later, with early dark energy fraction Ω_e free to go up to about 5% at 2 sigma if the onset of EDE happens at $z \lesssim 100$. Tight bounds around 1 – 2% are obtained whenever dark energy is present at last scattering, even if its effects switch off afterwards. We show that the CMB mainly constrains the presence of Dark Energy at the time of its emission, while EDE-modifications of the subsequent growth of structure are less important.

I. INTRODUCTION

Models of dynamical dark energy or quintessence [1, 2] can be roughly divided into two classes: with or without early dark energy (EDE). Models without early dark energy have a cosmology that is indistinguishable from a cosmological constant (Λ CDM) for a redshift larger than a few. Dark energy simply plays no role in early epochs of the universe. Usually, this class of models shares the same fine tuning and "why now" problems as Λ CDM. On the other hand, models with early dark energy are characterized by a non-negligible amount of dark energy at early times, that distinguishes them from Λ CDM: they can be related to a scaling or attractor solution where the fraction of dark energy follows the fraction of the dominant matter or radiation component [1]. As a consequence of the scaling behavior, such models predict in early cosmology a non-vanishing dark energy fraction Ω_e . Since Ω_e must be substantially smaller than the present dark energy fraction this class of models needs an "exit mechanism" explaining why the scaling solution ends in the recent cosmological past, such that the fraction in dark energy increases subsequently, leading to the observed accelerated expansion epoch. A large class of models of this type has been proposed. An example is growing neutrino quintessence [3, 4]. Such models may be very close to Λ CDM in the present and recent cosmological epoch, but have a nonzero Ω_e as a distinctive feature.

The central quantity for EDE is Ω_e , which measures the amount of dark energy present at early cosmological epochs. It is therefore natural to use this quantity for a parametrization of the time history of dark energy. This was done in refs.[5], where the name "early dark energy" was proposed and in subsequent works along this line [6]. Besides Ω_e these parametrizations use, as usual, Ω_m (from which $\Omega_{de} = 1 - \Omega_m - \Omega_r$ is derived) plus the present dark energy equation of state parameter w_0 . While the equation of state puts emphasis on how fast the dark energy fraction $\Omega_{de}(z)$ gets small as z increases, Ω_e measures how much dark energy is present at high z . The parametrization used in refs.[6–9] (EDE1) is illustrated in the left panel of Fig. 1. This behavior differs from Λ CDM, that can be seen as the approximate limit in which $\Omega_e \rightarrow 0$. Measuring how Ω_e differs from zero represents therefore a valuable tool to distinguish, and possibly falsify, a cosmological constant scenario from dynamical dark energy.

Bounds on the value of Ω_e have been found from various observations as nucleosynthesis [1, 10, 11], structure formation [12–14] or the separation of peaks in the CMB anisotropies [15]. The most precise bounds on EDE (or "early quintessence" as used in [14, 16]) arise from the analysis of CMB-anisotropies [7–9, 16, 17]. In particular, very severe bounds $\Omega_e \lesssim 0.02$ at 95% confidence for EDE1 have been found in the analysis of SPT-data by Reichard et al. [8], a factor of three improvement over WMAP7 data alone. Similarly, the recent [9] limits $\Omega_e < 0.025$ from WMAP7+ACT+ACTDefl at 95% confidence level. Such an improvement mostly comes from including CMB data at small angular scales, extending previous measurements of the temperature power spectrum (WMAP7, [18]) down to $\ell \sim 3000$, with first compelling evidence of CMB lensing [19, 20]. The impact of small-scale CMB measurements and gravitational lensing on cosmology is quite significant [21] and can indeed be used to constrain cosmological parameters. In particular, CMB lensing can be used to distinguish among different dark energy models [22–27].

Using updated data from WMAP [28] and SPT [29], we perform here an analysis similar to ref.[8] with emphasis on which cosmological period or redshift range the bounds apply: that is to say, how early is early? We confirm the analysis of [8] if Ω_e is constant for all redshifts $z \gtrsim 3$, while we find that the bounds are considerably weaker if the

effect of EDE is restricted to a limited range in z . After last scattering the main effect of EDE is a reduced growth of structure. This could be compensated by an enhancement of the growth rate due to other phenomena. An example is the growth of neutrino lumps in growing neutrino quintessence [30, 31]. Thus bounds on EDE for the period after last scattering have to be handled with care. On the other hand, a presence of dark energy during the period of last scattering mainly influences the evolution of geometry with much less possibilities of compensation.

Early dark energy parametrizations grab features of a large class of dynamical dark energy models, namely having a non-negligible fraction of dark energy at early times. The amount of early dark energy influences CMB peaks in various ways and can be strongly constrained when including small scale measurements. We here investigate whether CMB constraints are affected by a variation of the epoch when Ω_e is non negligible. In particular, we aim at distinguishing between two EDE-effects. The first is the reduced structure growth in the period after last scattering. This implies a smaller number of clusters as compared to Λ CDM, and therefore a weaker lensing potential influencing the anisotropies at high ℓ . We “isolate” this effect by “switching on” EDE only after last scattering, at a scale factor a_e . This is achieved by our parametrization EDE3. The second effect is the influence on the position and height of peaks arising from dark energy present at the epoch of last scattering [15]. This effect is “isolated” by our parametrization EDE4 for which EDE is present until a final scale factor a_f and switched off afterwards. Of course, the “isolation” is not perfect - the different parametrizations merely put particular emphasis on certain features.

We discuss in detail the differences between four EDE parametrizations, analyzing the effect of EDE on the CMB temperature power spectrum for each of them. The first parametrization (EDE1) is the one adopted by [6] and tested in [8]. The second, new, parametrization (EDE2) uses only two parameters instead of three, namely Ω_e and Ω_{m0} , without using w_0 as a third parameter as it happens for EDE1. It keeps Ω_e constant in the past, as for EDE1, but has a sharper transition from a non negligible EDE to Λ CDM. Incidentally, we note that such a sharp transition is effectively realized for growing neutrino quintessence cosmologies [3, 31, 32]. We find only small differences between EDE1 and EDE2, despite the absence of w_0 in EDE2. This also shows that the influence of the equation of state w_0 on the bound for Ω_e is small. The third and fourth parametrizations (EDE3 and EDE4), on which most of our analysis and results are focused, are also proposed here for the first time and they are used as a simple, yet powerful, tool to evaluate which epoch is most relevant for EDE constraints.

This paper is organized as follows. In Section II we review early dark energy and introduce the parametrizations used throughout the paper. In Section III we recall the basics of CMB lensing and the effects of EDE on the CMB lensing potential. In Section IV we illustrate the methods used, MonteCarlo simulations, parameters adopted and data. Our results are described in section V and conclusions drawn in Section VI.

II. EARLY DARK ENERGY

The presence of a non negligible amount of dark energy at early times is a quite generic feature present in several dynamical dark energy models. As such, it is interesting to understand how much EDE can be present and at which epochs, given our present knowledge of CMB measurements. Our aim is to evaluate the impact of EDE on CMB, identifying the effect that it has at different epochs of the evolution of the Universe. For this purpose, we consider here four classes of different EDE models. In Fig.(1) we show the evolution of the dark energy fraction for the four EDE parametrizations plus EDE0, which corresponds to the first proposal of an EDE parametrization [5]. In Fig.(2) we plot the corresponding equation of state.

A. EDE 0

This is the first EDE parametrization which was proposed in [5]. Here

$$\Omega_{de}(a) = \frac{e^{R(y)}}{1 + e^{R(y)}} , \quad (1)$$

where $y \equiv -\ln a$ and $R(y)$ is obtained as

$$R(y) = R_0 + \frac{3w_0 y}{1 + by} . \quad (2)$$

The constant R_0 is directly related to Ω_M by:

$$R_0 = \ln \left(\frac{1 - \Omega_M}{\Omega_M} \right) , \quad (3)$$

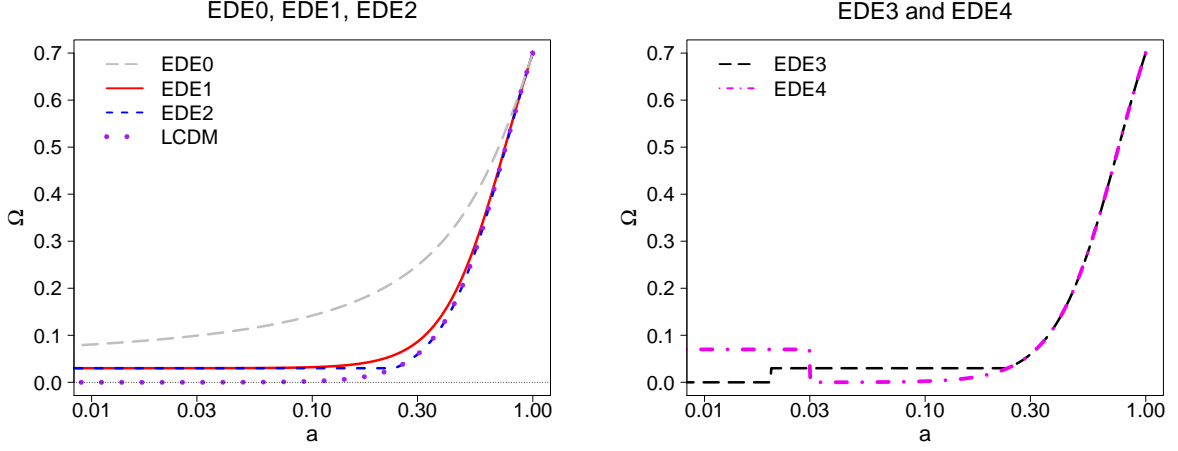


Figure 1: Dark energy density ratio with respect to the critical density vs the scale factor a . Left panel: EDE0 (long dashed grey), EDE1 (solid red) and EDE2 (dashed blue) for the same choice $\Omega_e = 0.03$. Λ CDM is also shown for comparison (dotted purple). Right panel: EDE3 (solid black), with $\Omega_e = 0.03$ and $a_e = 0.02$ is shown together with EDE4 (dot-dashed pink) for $a_f = 0.03 < a_c$ and $\Omega_e = 0.07$.

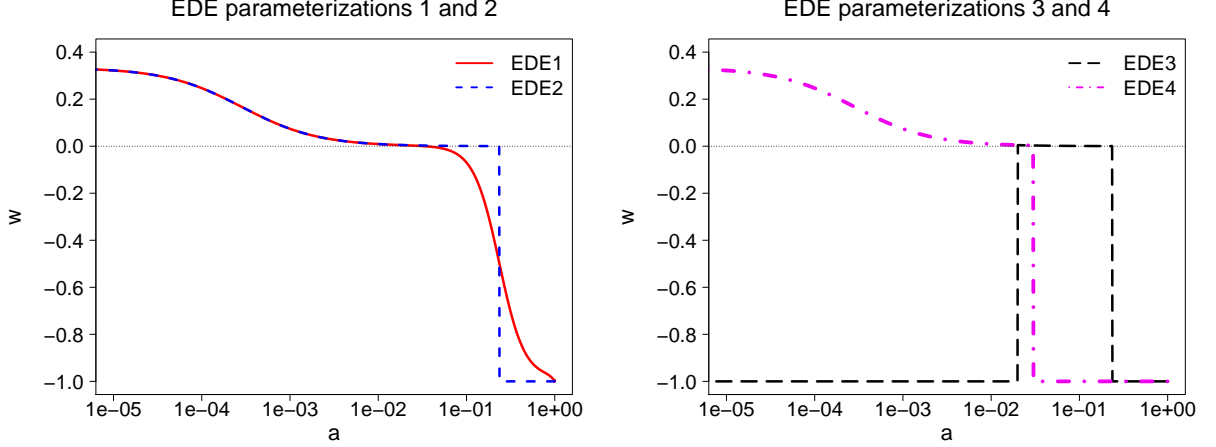


Figure 2: Dark energy equation of state $w(a)$ as a function of the scale factor a . Left panel: EDE1 (solid red) and EDE2 (dashed blue) for the same choice of the Ω_e parameter ($\Omega_e = 0.03$). Right panel: EDE3 (long dashed black) and EDE4 (dot-dashed magenta) for $\Omega_e = 0.03$ and $\Omega_e = 0.07$ respectively.

w_0 is the present equation of state for dark energy and b is a parameter that can be related to the amount of early dark energy Ω_e :

$$b = -\frac{3w_0}{\ln\left(\frac{1-\Omega_e}{\Omega_e}\right) + \ln\left(\frac{1-\Omega_M}{\Omega_M}\right)} . \quad (4)$$

In the limit in which $\Omega_e \rightarrow 0$ and $a \rightarrow 1$, the parameter $b \rightarrow 0$ and the model reduces to Λ CDM. If $b \neq 0$ there is a very smooth transition from Λ CDM to a model with a non negligible amount of dark energy at early times. The behavior of Ω_{de} for this parametrization is plotted in Fig.1. We will not use this parametrization in the following but it is interesting to compare its behavior with the sharper transition that characterizes the other parametrizations described below.

B. EDE 1

The first parametrization that we investigate numerically (EDE1) is the one proposed in [6] and tested in refs.[7–9]. The dependence of the dark energy fraction, Ω_{de} , on the scale parameter a is given by

$$\Omega_{de}(a) = \frac{\Omega_{de}^{(0)} - \Omega_e(1 - a^{-3w_0})}{\Omega_{de}^0 + \Omega_m^0 a^{3w_0}} + \Omega_e(1 - a^{-3w_0}). \quad (5)$$

Eq. (5) uses three parameters, the present matter fraction Ω_{m0} , the early dark energy fraction Ω_e and the present dark energy equation of state w_0 , with $\Omega_{de0} = 1 - \Omega_{m0}$. For any given function $\Omega_{de}(a)$ the scale dependent equation of state $w(a)$ obtains as a simple derivative [33]

$$w(a) = -\frac{1}{3[1 - \Omega_{de}(a)]} \frac{d \ln \Omega_{de}}{d \ln a} + \frac{a_{eq}}{3(a + a_{eq})}, \quad (6)$$

where $a_{eq} \sim 3200$ is the scale factor at matter-radiation equality, while the energy density is given by

$$\rho_{de}(a) = \frac{\rho_{de0}}{a^3} \frac{\Omega_{de}}{\Omega_{de0}} \frac{\Omega_{de} - 1}{\Omega_{de0} - 1} \left(1 + \frac{a_{eq}}{a}\right) \frac{1}{1 + a_{eq}}. \quad (7)$$

C. EDE 2

The second parametrization (EDE2), that we propose here for the first time, reads as follows:

$$\Omega_{de}(a) = \begin{cases} \Omega_e & a < a_c \\ \frac{\Omega_{de0}}{\Omega_{de0} + \Omega_{m0} a^{-3} + \Omega_{r0} a^{-4}} & a \geq a_c \end{cases} \quad (8)$$

Here a_c is determined by continuity at a_c , such that (neglecting Ω_{r0}):

$$a_c = \left[\frac{\Omega_e \Omega_{m0}}{\Omega_{de0}(1 - \Omega_e)} \right]^{1/3}. \quad (9)$$

In this way Ω_e is the only additional parameter, beyond Ω_{m0} . This is a minimal parametrization of EDE. Similar to other two-parameter settings for dark energy, as the ones using Ω_{m0} and w_0 , it is useful if data allow only for a rough distinction of dynamical dark energy from Λ CDM. This second parametrization considers a somewhat sharper transition between a phase in which there is a constant Ω_e contribution and the epoch in which dark energy looks close to a cosmological constant. We recall that in models of growing neutrino quintessence [3, 4, 31, 32] explain the “why now” problem by a cosmological trigger event, namely neutrinos becoming non-relativistic; for such models one typically finds a rather sharp transition between the two epochs.

D. EDE 3

For the EDE3-parametrization EDE becomes important only for $a > a_e$. Beyond Ω_{m0} it has two parameters, Ω_e and a_e , according to

$$\Omega_{de}(a) = \begin{cases} \frac{\Omega_{de0}}{\Omega_{de0} + \Omega_{m0} a^{-3} + \Omega_{r0} a^{-4}} & a \leq a_e \\ \Omega_e & a_e < a < a_c \\ \frac{\Omega_{de0}}{\Omega_{de0} + \Omega_{m0} a^{-3} + \Omega_{r0} a^{-4}} & a > a_c \end{cases} \quad (10)$$

In this case, early dark energy is present in the time interval between $a_e < a < a_c$ while outside this interval it behaves as in Λ CDM. In that interval, there is a non negligible EDE contribution, whose amount is parametrized by Ω_e . As in EDE2, a_c is fixed by the continuity condition, so that the parameters characterizing this case are (Ω_e, a_e) , that is to say how much EDE there is and how long its presence lasted. We note that for $a_e \ll a_c$ one has $\Omega_{de}(a \leq a_e) \approx 0$.

E. EDE 4

The next parametrization we choose provides somehow complementary information with respect to EDE3. For the EDE4 parametrization,

$$\Omega_{de}(a) = \begin{cases} \Omega_e & a < a_f \\ \frac{\Omega_{de0}}{\Omega_{de0} + \Omega_{m0}a^{-3} + \Omega_{r0}a^{-4}} & a > a_f \end{cases}, \quad (11)$$

early dark energy is present from early times until the scale factor reaches the value a_f , while Λ CDM is recovered at later times. For $a_f \ll a_c$ the dark energy fraction almost drops to zero at a_f , as visible in Fig. 1. To be formally consistent, we use eq. (11) only for $a_f < a_c$, while for $a_f > a_c$ we employ EDE2, eq. (8). We are interested, however, only in the case $a_f < a_c$. The parameters characterizing this case are (Ω_e, a_f) , that is to say how much EDE there is and since when it started to be negligible.

III. CMB TEMPERATURE POWER SPECTRUM AND LENSING POTENTIAL

An increase in EDE decreases the amount of CDM in a way that differs from what one would obtain by simply increasing the number of radiation species, since dark energy and radiation decay differently in redshift. There are two main effects of EDE on the CMB spectrum. The first consists in the influence on CMB peaks of the amount of dark energy present at the epoch of last scattering, the second is the suppression of structure growth, implying a smaller number of clusters as compared to Λ CDM. These two effects are approximately isolated in the two parametrizations EDE3 and EDE4. The effect of different EDE parametrizations on the CMB temperature power spectrum is shown in Fig.(3). For good visibility we have chosen a large value $\Omega_e = 0.1$. For more realistic values as $\Omega_e = 0.03$ the difference to Λ CDM is barely visible. The second parametrization, EDE2, boosts the amplitude of peaks somewhat higher than for EDE1.

EDE in general also moves the peaks to higher or smaller multipoles since they change the Hubble function $H(z)$ (see [15] for a quantitative analysis). EDE1, EDE2 and EDE4 produce a $H(z)$ always higher or equal to Λ CDM, both before and after decoupling. This reduces both the sound horizon at decoupling and the angular-diameter distance to last scattering, but the angular-diameter distance reduction is proportionally smaller because the last phase is in all cases identical to Λ CDM. The net effect on the peak angular scale (which is essentially the ratio of the sound horizon to the CMB distance) is therefore to move it to smaller values, or higher multipoles. In the case of EDE3 with a_e larger than the decoupling epoch, however, the sound horizon does not change at all with respect to Λ CDM and therefore the only effect is a decrease of the angular-diameter distance to last scattering, which leads to smaller peak multipoles. This can be understood also in terms of the quantitative formula (3) in ref. [15]: the presence of EDE at the time of last scattering ($\Omega_{lss} = \Omega_e$ for EDE1,2,4) shifts the peaks to higher ℓ s, while the presence of EDE in the period afterwards increases the averaged equation of state \bar{w}_0 and shifts the peaks to lower ℓ s. This effect suggests that bounds on EDE will not only depend on some time averaged fraction of dark energy, but also on the detailed time history.

We discuss here briefly another potential effect, namely the reduction of the growth rate due to the presence of EDE. This results in a modified lensing potential.

The CMB coming from the last scattering surface (LSS) is bent by gravitational structures on the path towards us; this effect is called CMB-lensing [21, 34] and its observation has recently been claimed by the ACT and SPT teams [19, 20, 35]. The deflection angle is of the order of 2 arcminutes, which would correspond to small scales and $l > 3000$ multipoles, where CMB peaks are already damped by photon diffusion. However, deflection angles are correlated over degree scales, so that lensing can modify the scales of the acoustic peaks, the main effect being a smoothing of primary peaks and a transfer of power to larger multipoles. CMB gravitational lensing naturally depends on the growth of perturbations and on the gravitational potentials. As a consequence, it is a good way to probe the existence of dark energy [22–27, 36, 37] and has recently been used to reject $\Omega_{\Lambda CDM} = 0$ at more than 5σ from CMB alone [35]. Since EDE has a strong impact on the growth of structure CMB lensing can be a sensitive probe to it [8].

We recall here only the main features of CMB-lensing, which is not the main topic of this paper but quite important when dealing with EDE constraints. For more details we refer to [21]. In the Matter Dominated Era (MDE) the potentials encountered along the way are constant in the linear regime and the gradient of the potential causes a total deflection angle α given by:

$$\alpha = -2 \int_0^{\chi_*} d\chi \frac{f_K(\chi_* - \chi)}{f_K(\chi_*)} \nabla_{\perp} \Psi(\chi \hat{n}; \tau_0 - \chi), \quad (12)$$

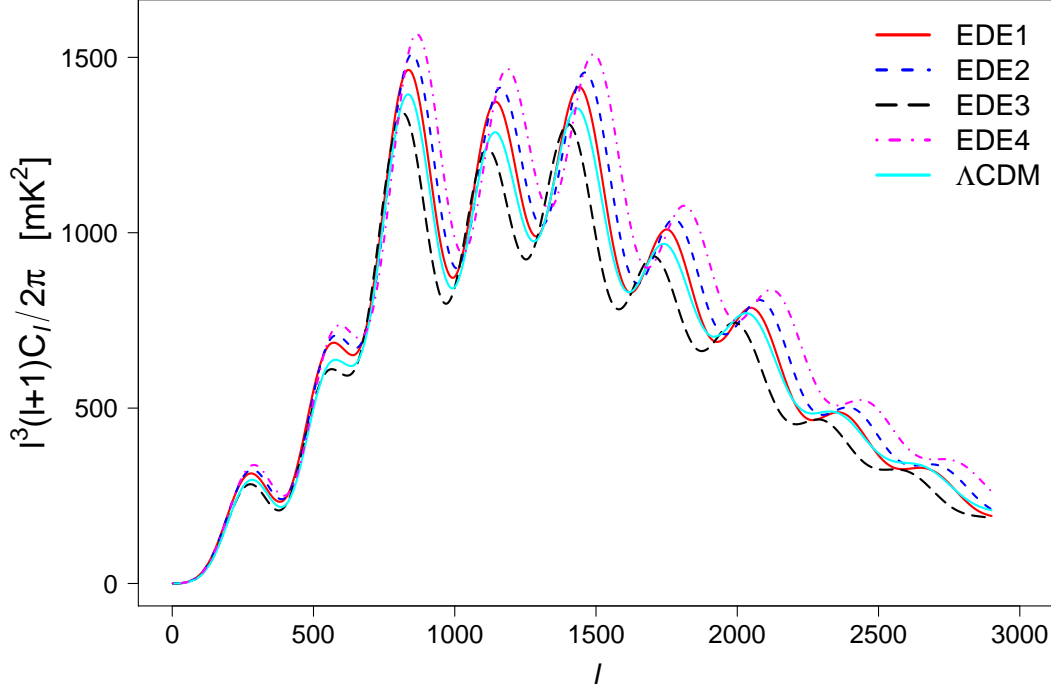


Figure 3: Temperature CMB power spectrum for four different EDE parametrizations. Here, in all cases, we have used a large value $\Omega_e = 0.1$ to show the effect of the different parametrizations. For smaller values, as $\Omega_e = 0.1$, the effect on the C_ℓ is quite small and smaller than the one on the lensing potential that we will see in Fig.4. EDE3 and EDE4 have $a_e = 0.02$ and $a_f = 0.03$ respectively. The Λ CDM spectrum is also shown for reference, for the same value of H_0 and Ω_{m0} today. Note that we are plotting $\ell^3(\ell+1)C_\ell/2\pi$ rather than $\ell(\ell+1)C_\ell/2\pi$.

where χ_* is the conformal distance of the source acting as a lens, Ψ is its gravitational potential, $\eta_0 - \chi$ is the conformal time at which the CMB photon was at position $\chi\hat{n}$. Here the function $f_K(\chi)$ is the angular diameter distance and it's equal to χ for a flat Universe, while it's a function of the curvature parameter K for non flat cosmologies [21].

The gravitational lensing potential ψ_ℓ is defined by

$$\psi_\ell(\hat{n}) \equiv -2 \int_0^{\chi_*} d\chi \frac{f_K(\chi_* - \chi)}{f_K(\chi_*)f_K(\chi)} \Psi(\chi\hat{n}; \eta_0 - \chi) . \quad (13)$$

The lensed CMB temperature $\tilde{T}_{\hat{n}}$ in a direction \hat{n} is given by the unlensed temperature in the deflected direction $\tilde{T}(\hat{n}) = T(\hat{n}') = T(\hat{n} + \alpha)$ where at lowest order the deflection angle $\alpha = \nabla\psi_\ell$ is just the gradient of the lensing potential. Expanding the lensing potential into spherical harmonics, one can define also the angular power spectrum C_ℓ^ψ corresponding to the lensing potential, defined as $\langle \psi_{\ell m} \psi_{\ell' m'}^* \rangle = \delta_{\ell\ell'} \delta_{mm'} C_\ell^\psi$. In Fig. 4 we show $C_{dd} \equiv [\ell(\ell+1)]^2 C_\ell^\psi / (2\pi)$ for different EDE parametrizations. Early Dark Energy reduces the lensing potential since structures grow less rapidly. For a given value Ω_e the reduction is stronger if EDE is present for a longer time, e.g. EDE1 and EDE2.

As we can see from Fig. 4, the CMB lensing potential mainly gives contribution to large scales or small ℓ up to $\ell \sim 1000$ or less. However, the lensed CMB temperature power spectrum depends on the convolution between the lensing potential and the unlensed temperature spectrum (see [21] for more details):

$$\tilde{C}_\ell^\Theta \approx (1 - \ell^2 R^\psi) C_\ell^\Theta + \int \frac{d^2\ell'}{(2\pi)^2} [\ell'(\ell - \ell')]^2 C_{|\ell - \ell'|}^\psi C_{\ell'}^\Theta , \quad (14)$$

where $R^\psi = 1/2 \langle |\nabla\psi|^2 \rangle$ is the total deflection angle power (typically of the order of $\sim 10^{-7}$), ℓ is the multipole, \tilde{C}_ℓ^Θ is the lensed temperature power spectrum, C_ℓ^Θ is the unlensed temperature power spectrum and C_ℓ^ψ is the lensing

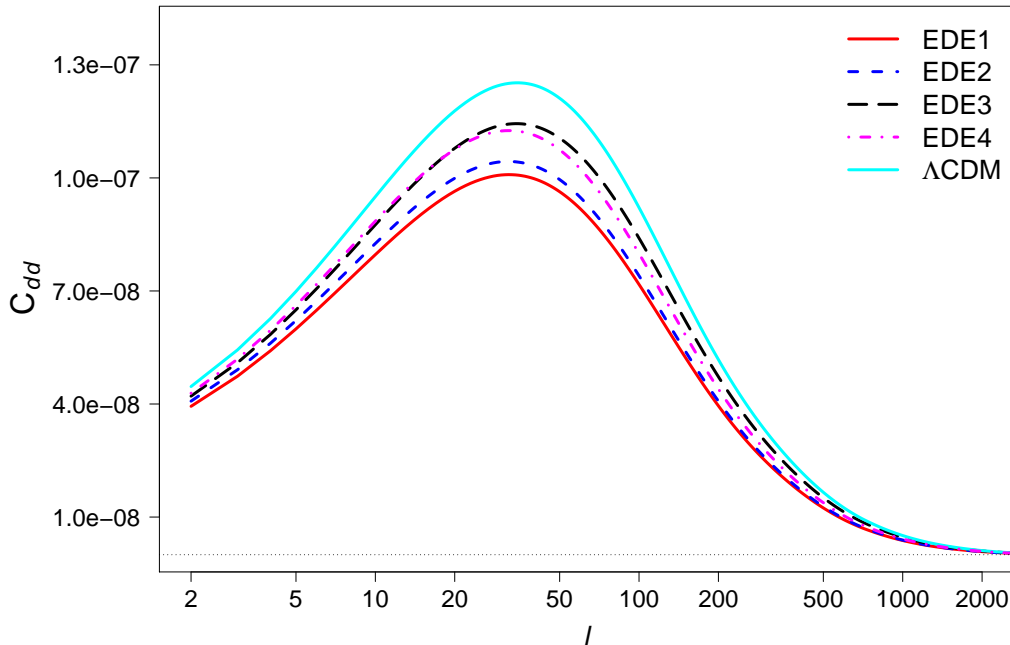


Figure 4: Dimensionless lensing potential $C_{dd} \equiv [\ell(\ell+1)]^2 C_\ell^{\psi} / (2\pi)$ versus multipole ℓ for different parametrizations. All EDE parametrizations correspond to a value of $\Omega_e = 0.03$, which is enough to see the differences in the lensing potential. EDE3 and EDE4 have $a_e = 0.02$ and $a_f = 0.03$ respectively. Λ CDM is also plotted for comparison (top-solid cyan).

potential. The resulting effect is of several percent at $\ell > 1000$, thus being important when estimating the spectrum up to small scales of $\ell \sim 3000$ as it happens for the SPT considered here. Also, the lensing depends on time, combining information from decoupling (from the last scattering surface of the CMB) and $z < 5$ (when large scale structures formed).

IV. METHODS

We have implemented each EDE parametrization in CAMB, joined to COSMOMC, in order to perform a Monte Carlo analysis and get information on the EDE parameters from present CMB measurements. We have compared theoretical predictions of CMB spectra with two datasets. The first includes WMAP9 temperature spectra [28], which updates results included in [8] (we have first also checked that we reproduced results in [8] using WMAP7). The second includes the latest South Pole Telescope spectrum [29, 35]. In order to use SPT data and compare our EDE results with the ones of [8, 29], we have installed the likelihood provided by the SPT team [19, 29] on the SPT website [41] and integrated it with the recommended version of cosmic [38] (August 2011). Bandpowers and foreground templates have been updated to [29]. Whenever including SPT data we also marginalize over the three nuisance parameters described in [19, 29]: two of them refer to Poisson point sources and clustered point sources; the third one adds power from the thermal and kinetic Sunyaev-Zel'dovich (SZ) effects. All these effects are relevant when small scales ($l \gtrsim 2000$) are included and must be therefore taken into account when SPT data are used.

For EDE1 and EDE2, the baseline set of parameters includes $\Theta = \Omega_b h^2, \Omega_c h^2, \theta_s, \log \mathcal{A}, n_s, \tau$ while Ω_{de0} is a derived parameter. In addition, when EDE is included two more parameters are added for EDE1: w_0, Ω_e , while EDE2 has one additional parameter Ω_e . For EDE1, we also investigated potential degeneracies with dark energy parameters: *case1* includes EDE1 with both WMAP and SPT; *case2* includes WMAP only; in *case3* we do not include lensing; in *case4* we marginalize over the effective number of relativistic species N_{eff} .

For EDE3 (EDE4), we fixed the optical depth to $\tau = 0.088$ in order to speed up the runs and we did several runs for different (fixed) values of a_e (a_f). This is enough for our purpose: we want to compare the two parametrizations and estimate the effect of this extra parameter, which gives information on how EDE bounds depend on the specific

Run	CMB-Lensing	WMAP9	SPT	Parameters
EDE1, case1	✓	✓	✓	baseline + $w_0 + \Omega_e$
EDE1, case2	✓	✓	X	baseline + $w_0 + \Omega_e$
EDE1, case3	X	✓	✓	baseline + $w_0 + \Omega_e$
EDE1, case4	✓	✓	✓	baseline + $w_0 + \Omega_e + N_{eff}$
EDE2	✓	✓	✓	baseline + Ω_e
EDE3	✓	✓	✓	baseline + Ω_e ; fixed τ and a_e
EDE4	✓	✓	✓	baseline + Ω_e ; fixed τ and a_f

Table I: Data and parameters for runs investigated in this paper. Note that unlike EDE1, the parametrizations EDE2, EDE3, EDE4 do not require the equation of state w_0 as an additional parameter.

Parameters and errors for EDE1

Parameter	case1	case2	case3	case4
$\Omega_b h^2$	0.022 ± 0.00035	0.023 ± 0.00060	0.021 ± 0.00033	0.023 ± 0.00049
$\Omega_c h^2$	0.11 ± 0.0039	0.11 ± 0.0053	0.11 ± 0.0041	0.13 ± 0.0087
θ_s	1.04 ± 0.0011	1.04 ± 0.0033	1.04 ± 0.00094	1.04 ± 0.0012
n_s	0.967 ± 0.0093	0.990 ± 0.018	0.950 ± 0.0095	0.995 ± 0.018
w_0	< -0.44	< -0.26	< -0.52	< -0.39
Ω_e	< 0.013	< 0.043	< 0.0098	< 0.012
N_{eff}	-	-	-	3.9 ± 0.51
Y_{He}	0.25 ± 0.00015	0.25 ± 0.00025	0.25 ± 0.00015	0.26 ± 0.0063
Ω_{de0}	0.64 ± 0.069	0.57 ± 0.091	0.65 ± 0.056	0.64 ± 0.071
H_0	62.0 ± 5.5	57.7 ± 6.2	62.9 ± 4.6	64.7 ± 6.2

Table II: Mean value plus standard deviation for a selection of baseline and derived parameters in EDE1. In the case of Ω_e and w we report the 95% confidence upper limit. Values of *case1* are compatible with [8]. Limits on Ω_e do not seem to be sensitive to marginalizing over the effective relativistic degrees of freedom N_{eff} .

time at which dark energy is present. Data and parameters of different runs are summarized in Tab.I.

V. RESULTS

A. Parametrizations 1 and 2

In tables II and III we compare the 1-sigma standard deviation for baseline and derived parameters for the various runs listed in Tab.I for the first two EDE parametrizations. The inclusion of SPT data (*case1*) improves the constraints on Ω_e with respect to WMAP9 only (*case2*), in agreement with results from [8] and updated to more recent data. This holds also for the second parametrization we propose here, with no significant difference for most of the parameters. If the second parametrization is adopted, however, constraints on derived parameters like Ω_{de} (and σ_8) improve of a factor of two, allowing though for a weaker constraint on the age of the Universe. No significant difference appears between *case1* and *case3* (no lensing) for the first parametrization (Tab.II). When we allow for the number of relativistic species to vary from the reference value $N_{eff} = 3.046$ we obtain results for the *case4* run: due to the degeneracy between N_{eff} , the spectral index, dark energy and matter parameters, constraints on n_s are wider by almost a factor 2, constraints on $\Omega_c h^2$ by a factor 2.5. Also, constraints on the Y_{He} widen by a factor of 41. No significant change, though, is seen on Ω_e . Similar results hold for both EDE parametrizations. This is clearly visible also from the 2D likelihood plots in fig.5 (also in agreement with [8] but updated to more recent data) where we have added marginalization over N_{eff} . The 2D likelihood plot for EDE2 looks very similar to the one for EDE1, so we do not show it. In conclusion we note that a steeper switch from Λ CDM to non negligible dark energy, as in EDE2, does not affect present bounds on Ω_e . In the next paragraph we analyze results from EDE3 and EDE4, which will help us understand which range in redshift determines the bounds on Ω_e .

Parameters and errors for EDE2

Parameter	case 1	case 2	case 4
$\Omega_b h^2$	0.022 ± 0.00035	0.023 ± 0.00051	0.023 ± 0.00047
$\Omega_c h^2$	0.11 ± 0.0039	0.12 ± 0.0053	0.12 ± 0.0086
θ_s	1.04 ± 0.0011	1.04 ± 0.0033	1.04 ± 0.0011
n_s	0.967 ± 0.0095	0.979 ± 0.013	0.99 ± 0.017
Ω_e	< 0.014	< 0.041	< 0.013
N_{eff}	-	-	3.8 ± 0.48
Y_{He}	0.25 ± 0.00015	0.25 ± 0.00021	0.26 ± 0.0060
Ω_{de}	0.74 ± 0.020	0.71 ± 0.029	0.75 ± 0.020
H_0	71.4 ± 1.7	69.5 ± 2.3	76.0 ± 3.5

Table III: Mean value (not best fit) plus standard deviation for a selection of baseline and derived parameters in EDE2. In the case of Ω_e and w we report the 95% confidence upper limit. Limits on Ω_e do not seem to be sensitive to marginalizing over the effective relativistic degrees of freedom N_{eff} .

B. Parametrizations 3 and 4

We now move to the runs using the parametrizations EDE3 and EDE4. For this test, it is sufficient to fix τ in both cases, as we are only interested in comparing results from EDE3 and EDE4 for different values of a_e and a_f . To do so, we consider EDE3 simulations for $a_e = (0.001, 0.01, 0.03, 0.1, 0.2)$ and EDE4 for $a_f = (0.003, 0.01, 0.03, 0.1, 0.2)$. In EDE3 we expect that for a_e sufficiently small, we recover EDE2 results, while for a_e approaching a_c we recover Λ CDM. In EDE4 we expect that for a_f small enough we recover Λ CDM while for a_f approaching a_c we obtain EDE2.

In Fig.6 we show 1D likelihoods for different values of a_e . For EDE3 we conclude that the bounds on Ω_e get weaker as the onset of EDE is delayed. The presence or absence of dark energy in a redshift range $z \approx 2 - 10$ is hard to be detected.

In Fig.7 we show best fit results for EDE3, at different values of a_e or equivalently $1 + z_e \equiv 1/a_e$. We recall that a_e indicates the time from which Dark Energy started to be non-negligible. We see, as expected, that for values of a_e close to CMB decoupling ($a \sim 0.001$) we approach limits found for EDE2. On the other side, for values of a_e closer to a_c , Dark Energy becomes non-negligible later, approaching a Λ CDM scenario: in this case we finally have no limits on Ω_e . Interestingly, for the first time we show the limits we actually have at intermediate a_e or z_e : these become less stringent the later Dark Energy starts to become non-negligible. In particular, for $a_e \sim 0.01 - 0.03$ (so if EDE becomes non negligible around $z \sim 40 - 60$) Ω_e is allowed to be as big as about 8% at 2 sigma from that time on. In Fig.8 we also show the mean value of Ω_e for different values of a_e . (For $z_e < 100$ the mean differs from zero at a bit more than one sigma.)

We recall that EDE3 and EDE4 are used here as a mean to isolate the two main effects that are caused by the presence of EDE. The first is the reduced structure growth in the period after last scattering; this implies a reduced number of clusters as compared to Λ CDM and therefore a weaker effect of the lensing potential on the CMB peaks. This first effect has been isolated through parametrization EDE3, by switching on EDE3 only after a_e . The second effect concerns the influence on the CMB peaks arising from the presence of dark energy at the epoch of last scattering. This second effect is isolated in parametrization EDE4, in which EDE only lasts until a final value $a = a_f$. In Fig.9 we plot the best fit results for EDE4, at different values of a_f or equivalently $1 + z_f \equiv 1/a_f$. For EDE4 the presence of dark energy during last scattering affects bounds at all times, independently of a_f . This shows that tight constraints on early dark energy come from the last scattering epoch rather than late time cosmology. Therefore if a non negligible amount of dark energy is present at CMB, constraints are almost independent of whether early dark energy switches off afterwards. The main CMB constraints in presence of EDE do not come then from the suppression of the growth of structures or from the late ISW but rather from its presence at last scattering.

VI. CONCLUSIONS

A constant fraction of early dark energy (EDE) reduces the growth rate over a large period and therefore has a substantial effect on the power spectrum of cosmic structures or the induced gravitational potential. If the growth rate is not affected by other properties of a model one can place strong constraints on such EDE models. Furthermore, the presence of EDE at the time of last scattering modifies the geometry and therefore influences the location and height of the CMB peaks. Again, this can be constrained by precision CMB data at large multipoles. For a simple

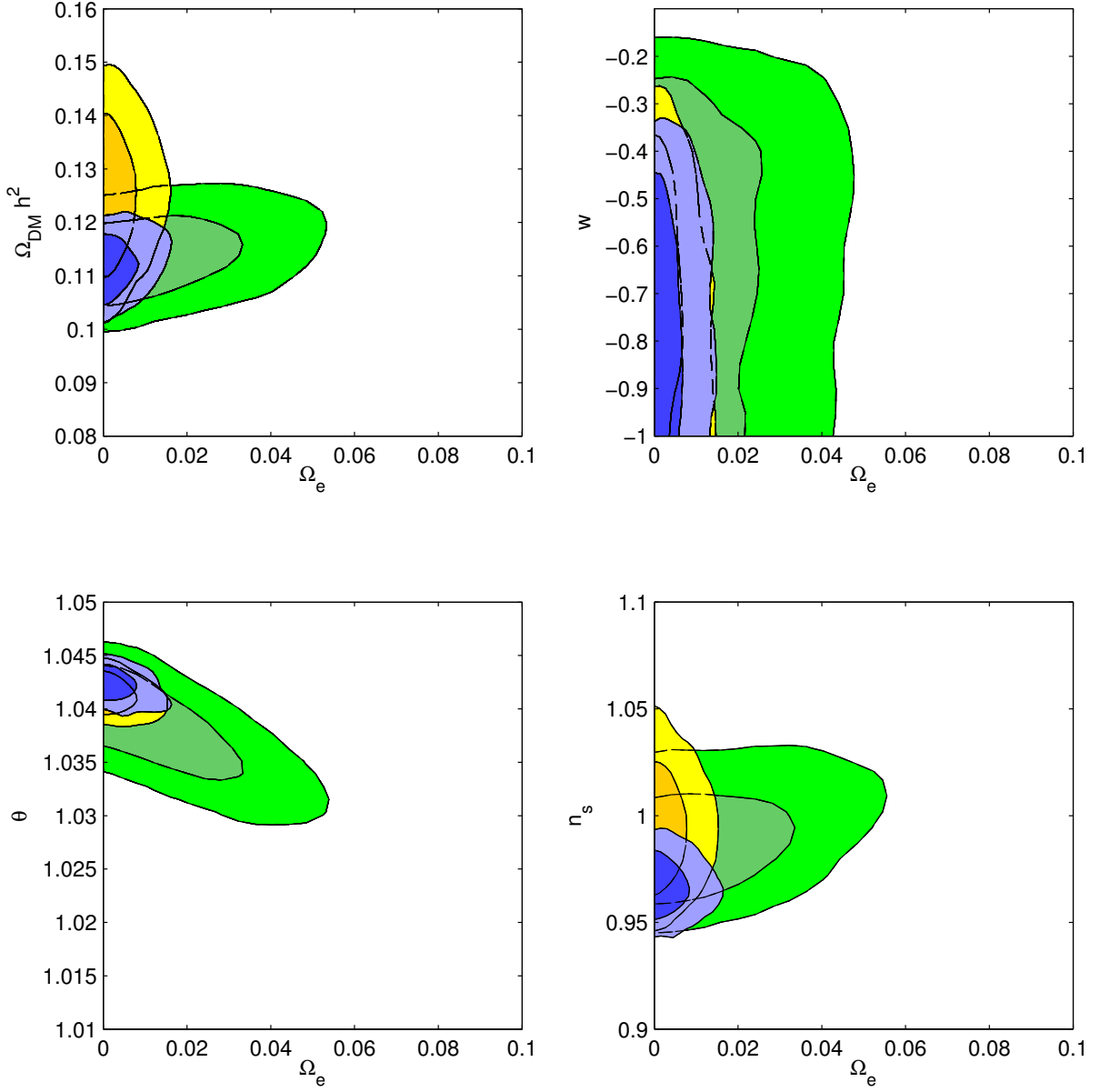


Figure 5: Confidence contours for the cosmological parameters for EDE1 models. We compare here run *case1* (WMAP9 + SPT, blue contours), *case2* (WMAP9 only, green contours), *case4* (WMAP9 + SPT, N_{eff} , yellow contours). 1 σ and 2 σ contours are shown.

parametrization of the time evolution of dark energy involving only two parameters, namely the fraction of dark energy at present $\Omega_{de0} = 1 - \Omega_{m0}$, and the constant fraction of dark energy at early times, Ω_e , we find a constraint $\Omega_e < 0.015$ at 95% confidence level.

On the other hand, our detailed analysis reveals that the assumptions of constant Ω_e and the absence of other factors influencing the growth rate has a very strong impact on the constraint. If the onset of EDE is delayed, starting only for a scale factor a_e , the bounds get much weaker, $\Omega_e < 0.08$ for $a_e \approx 0.02$. Furthermore, our analysis shows that the main constraints on EDE come from the last scattering epoch rather than from the suppression of the subsequent growth of structure. We have mimicked this by the EDE4 simulation for which dark energy is always present at last scattering but becomes absent for $z < z_f$ that we have tested up to $1 + z_f = 300$ with no effect on the bounds. Our parametrization EDE4, compared to EDE1, shows that even if the lensing potential is different for these two parametrizations, constraints remain similar. This seems to indicate that gravitational lensing is not the main source of information for Early Dark Energy bounds. This finding appears to be in agreement with *case3* of EDE1, in which lensing was switched off.

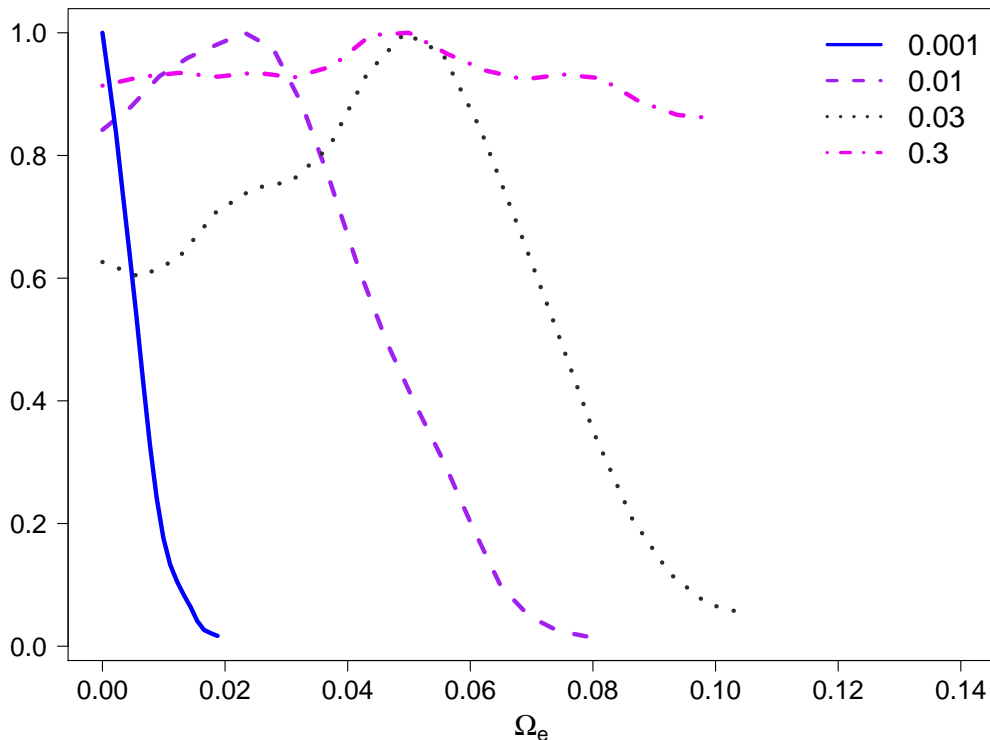


Figure 6: 1D likelihoods for the cosmological parameters for EDE3 for four values of a_e . As expected, for a_e sufficiently large, we get no constraint on Ω_e as we approach the Λ CDM scenario.

We recall that realistic models in which early dark energy is present, usually also have other effects which accompany the presence of a non negligible amount of dark energy in the background. Typically, dark energy models also affect clustering (ex. coupled quintessence, growing neutrinos, or any form of 'clustering' dark energy). The growth of structures will remain an important source of information constraining dark energy models via other probes such as weak lensing and baryonic acoustic oscillations [39, 40].

Finally, we have proposed the new parametrization EDE2, similar to EDE1 but with a sharper transition in $\Omega(a)$: this parametrization has the advantage of having one parameter less than EDE1 (w here is not a parameter). As bounds on Ω_e do not depend substantially on how sharp the transition is, EDE2 is good enough to picture a scenario in which early dark energy is present at all times. This may help to extract information about the time history of dark energy from limited data sets. In view of Figs. 7 and 8 it becomes clear, however, that bounds on Early Dark Energy depend crucially on the precise time history or on *how early is early*.

Acknowledgments

VP is supported by Marie Curie IEF, Project DEMO. L.A. and C.W. acknowledge support from DFG through the TRR33 program "The Dark Universe".

-
- [1] C. Wetterich, Nucl. Phys. **B302**, 668 (1988).
 - [2] B. Ratra and P. J. E. Peebles, Phys. Rev. **D37**, 3406 (1988).
 - [3] L. Amendola, M. Baldi, and C. Wetterich, Phys. Rev. **D78**, 023015 (2008), [arXiv:0706.3064](#).
 - [4] C. Wetterich, Phys. Lett. **B655**, 201 (2007), [arXiv:0706.4427](#).
 - [5] C. Wetterich, Phys.Lett. **B594**, 17 (2004), [arXiv:astro-ph/0403289](#).

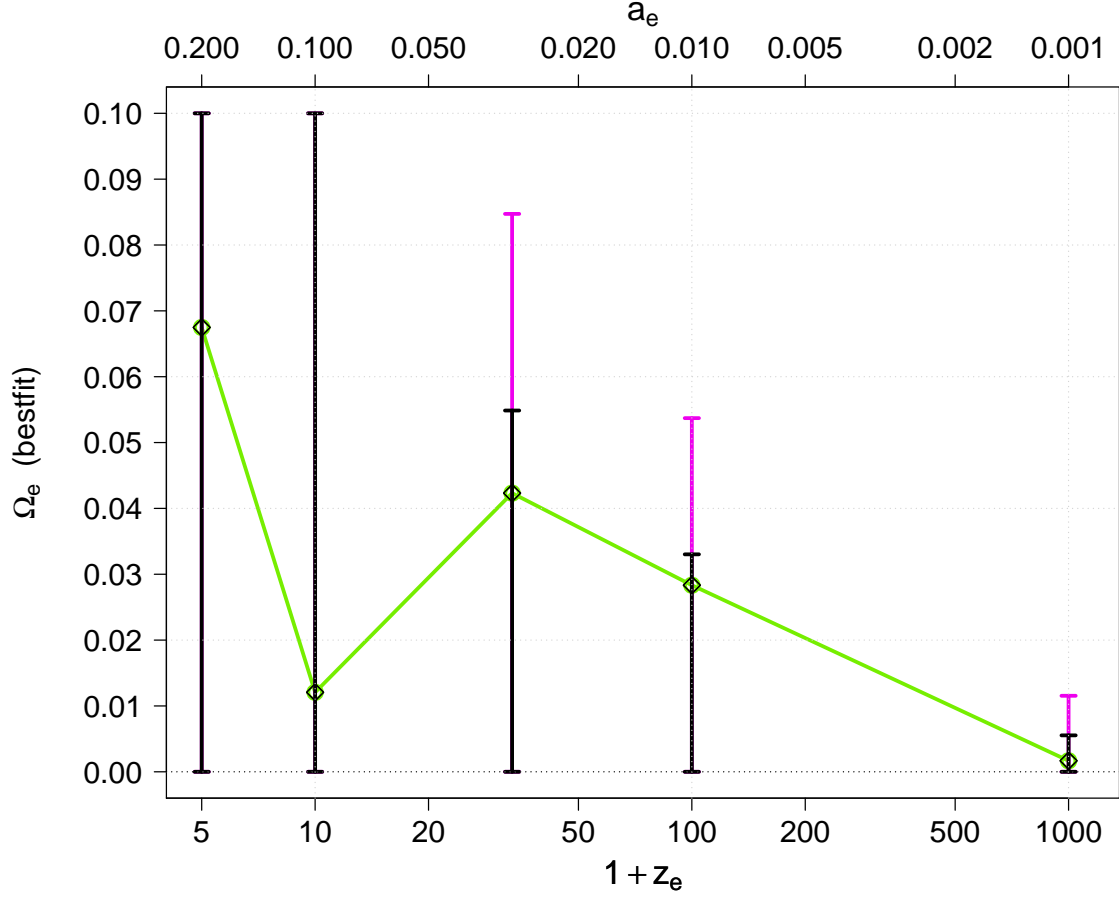


Figure 7: Bestfit for Ω_e EDE3 as a function of $1 + z_e \equiv 1/a_e$. Error bars correspond to 1 sigma (black) and 2 sigma (magenta) marginalized limits (upper1 and lower1, upper2 and lower2) respectively. The prior on Ω_e in the runs is $[0 : 0.1]$ so the error bars of the first two points are saturated. This shows that for values of z_e close to last scattering, bounds are confirmed to be tight; for $1 + z_e \sim 5$, or equivalently $a_e = 0.2$, we are close to a Λ CDM scenario; in the range in between, for $a_e \sim 0.01 - 0.03$ (for which EDE becomes non negligible around $z \sim 40 - 100$) Ω_e is less constrained and can be as high as 8% at 2 sigma from that time on. The top axis shows the corresponding values for a_e .

- [6] M. Doran and G. Robbers, JCAP **0606 (2006) 026** (2006).
- [7] E. Calabrese, R. de Putter, D. Huterer, E. V. Linder, and A. Melchiorri, *Phys. Rev. D* **83**, 023011 (2011), [arXiv:1010.5612](#).
- [8] C. L. Reichardt, R. de Putter, O. Zahn, and Z. Hou, *ApJ* **749 (2012) L9** (2012), [arXiv:1110.5328](#).
- [9] J. L. Sievers, R. A. Hlozek, M. R. Nolta, V. Acquaviva, G. E. Addison, P. A. R. Ade, P. Aguirre, M. Amiri, J. W. Appel, L. F. Barrientos, et al., *ArXiv e-prints* (2013), [arXiv:1301.0824](#).
- [10] M. Birkel and S. Sarkar, *Astropart.Phys.* **6**, 197 (1997), [arXiv:astro-ph/9605055](#).
- [11] R. Bean, S. H. Hansen, and A. Melchiorri, *Phys.Rev.* **D64**, 103508 (2001), [arXiv:astro-ph/0104162](#).
- [12] P. G. Ferreira and M. Joyce, *Phys.Rev.Lett.* **79**, 4740 (1997), [arXiv:astro-ph/9707286](#).
- [13] P. G. Ferreira and M. Joyce, *Phys.Rev.* **D58**, 023503 (1998), [arXiv:astro-ph/9711102](#).
- [14] M. Doran, J.-M. Schwindt, and C. Wetterich, *Phys.Rev.* **D64**, 123520 (2001), [arXiv:astro-ph/0107525](#).
- [15] M. Doran, M. J. Lilley, J. Schwindt, and C. Wetterich, *Astrophys.J.* **559**, 501 (2001), [arXiv:astro-ph/0012139](#).
- [16] R. R. Caldwell, M. Doran, C. M. Mueller, G. Schafer, and C. Wetterich, *Astrophys.J.* **591**, L75 (2003), [arXiv:astro-ph/0302505](#).
- [17] M. Doran, M. Lilley, and C. Wetterich, *Phys.Lett.* **B528**, 175 (2002), [arXiv:astro-ph/0105457](#).
- [18] E. Komatsu, K. M. Smith, J. Dunkley, C. L. Bennett, B. Gold, G. Hinshaw, N. Jarosik, D. Larson, M. R. Nolta, L. Page, et al., *The Astrophysical Journal Supplement Series* **192**, 57 (2010), [arXiv:1001.4538v3\[astro-ph.CO\]](#).
- [19] R. Keisler, C. Reichardt, K. Aird, B. Benson, L. Bleem, et al., *Astrophys.J.* **743**, 28 (2011), [arXiv:1105.3182](#).
- [20] S. Das, B. D. Sherwin, P. Aguirre, J. W. Appel, J. Bond, et al., *Phys.Rev.Lett.* **107**, 021301 (2011), [arXiv:1103.2124](#).
- [21] A. Lewis and A. Challinor, *Physics Reports* **429**, 1 (2006), [arXiv:arXiv:astro-ph/0601594](#).

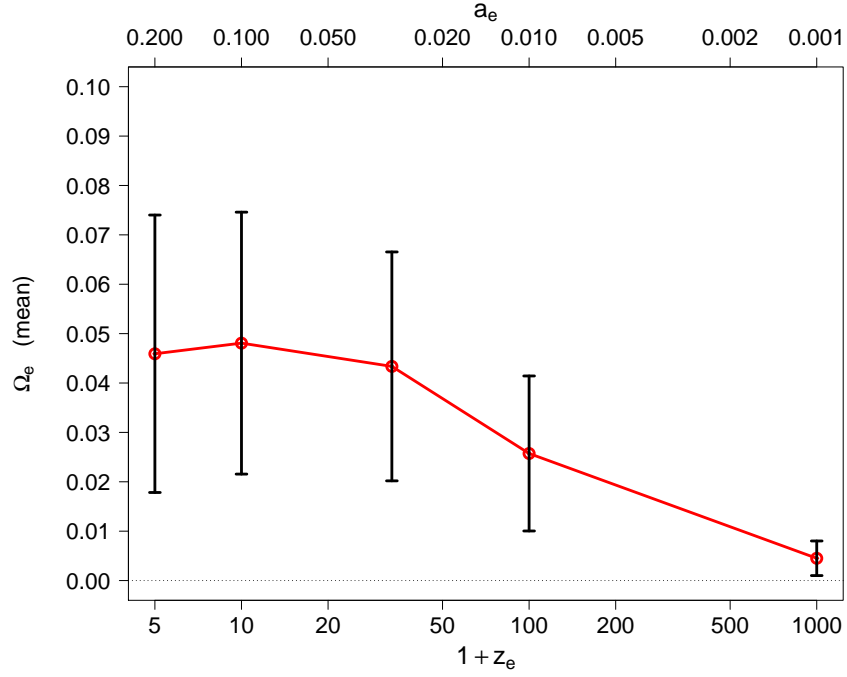


Figure 8: Mean plus/minus standard deviation for Ω_e EDE3 as a function of $1+z_e \equiv 1/a_e$.

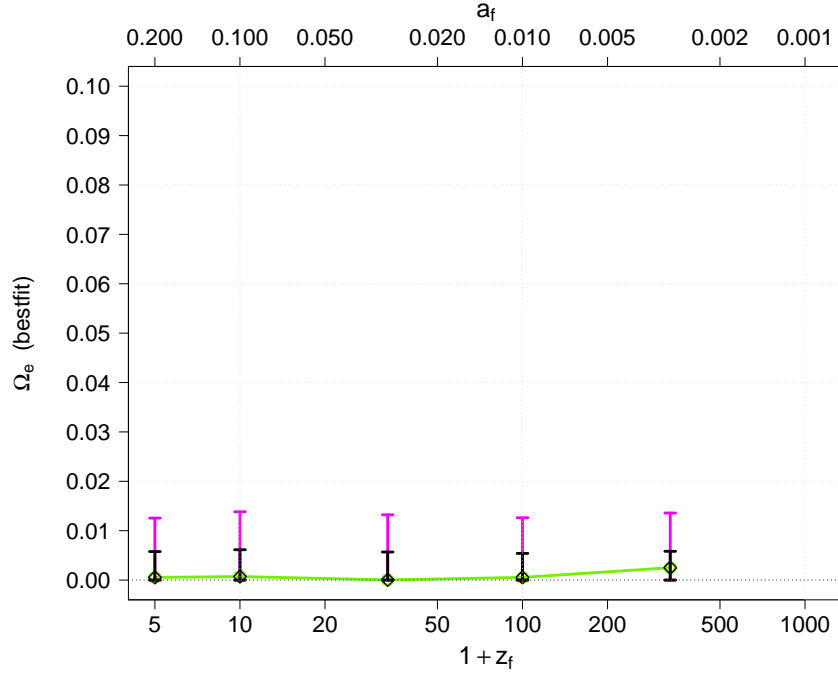


Figure 9: Bestfit for Ω_e EDE4 as a function of $1+z_f \equiv 1/a_f$. Error bars correspond to 1 sigma (black) and 2 sigma (magenta) marginalized limits (upper1 and lower1, upper2 and lower2) respectively. This shows that tight constraints on early dark energy come from CMB rather than late time cosmology so that if a non negligible amount of dark energy is present at CMB, constraints are almost independent of whether early dark energy switches off afterwards. The main CMB constraints in presence of EDE do not come from the suppression of the growth of structures or from the late ISW but rather from its presence at last scattering. The top axis shows the corresponding values for a_f .

- [22] L. Verde and D. N. Spergel, *Phys. Rev. D* **65**, 043007 (2002), URL <http://link.aps.org/doi/10.1103/PhysRevD.65.043007>.
- [23] F. Giovi, C. Baccigalupi, and F. Perrotta, *ArXiv Astrophysics e-prints* (2003), [arXiv:arXiv:astro-ph/0309422](#).
- [24] V. Acquaviva and C. Baccigalupi, *Phys. Rev. D* **74**, 103510 (2006), [arXiv:arXiv:astro-ph/0507644](#).
- [25] V. Acquaviva, C. Baccigalupi, and F. Perrotta, *Phys. Rev. D* **70**, 023515 (2004), [arXiv:arXiv:astro-ph/0403654](#).
- [26] W. Hu, D. Huterer, and K. M. Smith, *Astrophys. J. Lett.* **650**, L13 (2006), [arXiv:arXiv:astro-ph/0607316](#).
- [27] B. D. Sherwin, J. Dunkley, S. Das, J. W. Appel, J. Bond, et al., *Phys.Rev.Lett.* **107**, 021302 (2011), [arXiv:1105.0419](#).
- [28] G. Hinshaw, D. Larson, E. Komatsu, D. N. Spergel, C. L. Bennett, J. Dunkley, M. R. Nolta, M. Halpern, R. S. Hill, N. Odegard, et al., *ArXiv e-prints* (2012), [arXiv:1212.5226](#).
- [29] Z. Hou, C. L. Reichardt, K. T. Story, B. Follin, R. Keisler, K. A. Aird, B. A. Benson, L. E. Bleem, J. E. Carlstrom, C. L. Chang, et al., *ArXiv e-prints* (2012), [arXiv:1212.6267](#).
- [30] N. Wintergerst, V. Pettorino, D. F. Mota, and C. Wetterich, *Phys. Rev.* **D81**, 063525 (2010), [arXiv:0910.4985](#).
- [31] V. Pettorino, N. Wintergerst, L. Amendola, and C. Wetterich (2010), [arXiv:1009.2461](#).
- [32] D. F. Mota, V. Pettorino, G. Robbers, and C. Wetterich, *Phys. Lett.* **B663**, 160 (2008), [arXiv:0802.1515](#).
- [33] C. Wetterich (2003), [arXiv:hep-ph/0302116](#).
- [34] M. Bartelmann and P. Schneider, *Phys. Rept.* **340**, 291 (2001), [arXiv:astro-ph/9912508](#).
- [35] K. T. Story, C. L. Reichardt, Z. Hou, R. Keisler, K. A. Aird, B. A. Benson, L. E. Bleem, J. E. Carlstrom, C. L. Chang, H. Cho, et al., *ArXiv e-prints* (2012), [arXiv:1210.7231](#).
- [36] V. Pettorino, L. Amendola, C. Baccigalupi, and C. Quercellini (2012), [arXiv:1207.3293](#).
- [37] L. Amendola, V. Pettorino, C. Quercellini, and A. Vollmer, *Phys. Rev. D* **85**, 103008 (2012), [arXiv:1111.1404](#).
- [38] A. Lewis and S. Bridle, *Phys. Rev. D* **66**, 103511 (2002), [arXiv:arXiv:astro-ph/0205436](#).
- [39] L. Amendola, S. Appleby, D. Bacon, T. Baker, M. Baldi, N. Bartolo, A. Blanchard, C. Bonvin, S. Borgani, E. Branchini, et al., *ArXiv e-prints* (2012), [arXiv:1206.1225](#).
- [40] Euclid Consortium, <http://sci.esa.int/science-e/www/object/index.cfm?fobjectid=48983#> (2011).
- [41] <http://pole.uchicago.edu/public/data/keisler11/index.html>